EXPERIMENTAL STUDY ON SEISMIC PERFORMANCE OF SPRIAL STEEL PIPES

Kiyoshi Ono[1], Mitsuyoshi Akiyama[2] and Atsushi Yabumoto[3]

Abstract

It has been required to decrease the construction cost of infrastructures. The application of spiral steel pipes to bridge piers is considered as one of the effective methods. Spiral steel pipes are relatively economical because they are produced in large quantities in factories. However, mechanical features of spiral steel pipes including seismic performance may be different from those of bending roll pipes. In this study, cyclic loading experiments were conducted for grasping the elasto-plastic behavior of spiral steel pipes. Furthermore, the experimental results were compared with previous experimental results and analysis results by the previous seismic evaluation methods.

Introduction

It has been required to decrease the construction cost of infrastructures and a lot of attempts have been conducted for reducing construction cost. As one of the effective methods, the application of spiral steel pipes to bridge piers is considered. Spiral steel pipes have been seldom used for highway bridge piers. Spiral steel pipes have been commonly used as steel pipe piles of buildings or bridges. The spiral steel pipes are manufactured in factories by continually unwinding coils and molding them spirally into pipes, with the joints being automatically welded. This enables production in large quantities, making spiral steel pipes relatively economical. However, roll forming processes of spiral steel pipes are different from those of bending roll pipes which are generally used as steel bridge piers. For this reason, mechanical features and fatigue strength of spiral steel pipes may be different from those of bending roll pipes (Kimura et al. 2001). Therefore, it is very important to grasp them in order to establish a new design method for the spiral steel pipes.

In this study, elasto-plastic behavior of spiral steel pipes was focused on as the mechanical behavior. In order to grasp the elasto-plastic behavior of spiral steel pipes, cyclic loading experiments with two specimens were conducted. On the basis of the experimental results, the seismic performance of spiral steel pipes was investigated. Furthermore, the experimental results were compared with the previous experimental results of bending roll pipes and the analysis results by the previous seismic evaluation methods for bending roll pipe piers.

[1]Associate Professor, Department of Civil Engineering, Tokyo Institute of Technology.
[2]Associate Professor, Department of Civil Engineering, Tohoku University.
[3]Graduate Student, Department of Civil Engineering, Osaka University.

Outline of Experiments

(1) Test Specimen

In this investigation, two test specimens were employed. The outline of the dimensions of test specimen is given in Figure 1 and the values of major parameters of the test specimens are listed in Table 1. The test specimens were made in SKK490. SKK490 has been commonly employed as steel pipe piles. The values of the radius thickness ratio parameter applied to each specimen were different. The plate thicknesses of test specimens A9-P and A7-P are 9mm and 7mm, respectively. R_t is a radius thickness ratio parameter. $\overline{\lambda}$ is a slenderness ratio parameter of the column. The definitions of parameters mentioned above are identical to those stipulated in the 2002 design specifications (Japan Road Association 2002a; Japan Road Association 2002b) and given as follows.

$$R_t = \sqrt{3\left(1-\nu^2\right)}\frac{\sigma_y}{E}\frac{D}{2t} \tag{1}$$

$$\overline{\lambda} = \frac{1}{\pi}\sqrt{\frac{\sigma_y}{E}}\frac{2h}{r} \tag{2}$$

where D = diameter; t = plate thickness; σ_y = yield stress gained from material experiment; E = Young's modulus; ν = Poisson's ratio; h= column height (distance from the bottom of the column to the point of application of horizontal load); r = radius of gyration of cross section.

(2) Loading Condition

Each specimen was loaded with hydraulic jacks that were installed in a fully stiff frame as shown in Figure 2. In each experiment, the specified axial force as shown in Table 1 was first applied to the specimen by the vertical hydraulic jack. The axial force in Table 1 is 15% of yield axial force calculated using the nominal yield stress.

The cyclic pattern of the horizontal displacement is schematically shown in Figure 3, where δ_{yN} is calculated by the following equation. The axial load was kept constant during the cyclic experiment.

$$P_{yN} = \left(\sigma_{yN} - \frac{N}{A}\right)\frac{Z}{h} \tag{3}$$

$$\delta_{yN} = \frac{P_{yN}h^3}{3EI} \tag{4}$$

where σ_{yN} = nominal yield stress; N = axial load during the cyclic experiment; I = moment of inertia; Z = section modulus.

Experimental Results and Comments

(1) Feature of Hysteretic Curves

Figure 4 shows horizontal load - horizontal displacement hysteretic curves and Figure 5 shows the normalized envelope curves of the hysteretic curves. The major values of experimental results are shown in Table 2. Definitions of symbols in Table 2 are illustrated in Figure 6 and their descriptions are as follows. P_{max} is a maximum horizontal load. δ_m is a horizontal displacement at P_{max}. P_{yM} is a yield horizontal load calculated by Eq. (3) with σ_{yM} instead of σ_{yN}. δ_{yM} is a yield horizontal displacement at P_{yM} calculated by Eq. (4) with P_{yM} instead of P_{yN}. δ_{yEM} is a yield horizontal displacement at P_{yM} by using the initial stiffness obtained from the experimental results. The triangular symbols (▲) in Figure 5 show the points where P_{max} was observed.

Figure 4 shows that the hysteretic loop size, P_{max} and δ_m decrease with the increase in the radius thickness ratio parameter. The same tendency can be observed in envelop curves in Figure 5. And this tendency agrees with that of bending roll pipes (Public Works Research Institute 1997-1999).

(2) Buckling Modes

Figure 7 shows the buckling mode of the test specimen A7-P and Figure 8 shows that of the test specimen A9-P at the base section after the experiments. Figure 9 and Figure 10 show the distribution of out-of-plane deformation along each vertical line of the test specimens A7-P and A9-P respectively. It is known by the previous study that the typical buckling mode of bending roll pipe piers is “elephant foot buckling”. The feature of “elephant foot buckling” is that out-of-plane deformation along the whole circumference is caused by buckling and the direction of the out-of-plane deformation is the outside of pipes (Public Works Research Institute et al.1997-1999). The buckling mode of the test specimen A7-P shown in Figure 7 was similar to that of bending roll pipes. On the other hand, it is found that the buckling mode of the test specimen A9-P shown in Figure 8 was different from that of bending roll pipes. It is thought that the difference in buckling modes may be affected by the welding seam of spiral steel pipes. However, it is impossible to identify the cause of the difference in buckling modes. In the future works, the reason why the buckling modes were different will be examined in detail.

Applicability of the Previous Seismic Evaluation Method

The comparison of experimental results of spiral steel pipes in this study with the previous experimental results of bending roll pipes and the analysis results by the previous seismic evaluation method for the bending roll steel pipes was conducted in order to verify whether the previous seismic design method can be applied to spiral steel pipes. P_{max} and δ_m were focused on as indexes for confirming the applicability of the previous evaluation method to the spiral steel pipes. The seismic evaluation method described in the 2002 seismic design specifications for highway bridges (Japan Road Association 2002b) was adapted as the previous seismic evaluation method.

In the 2002 seismic design specifications, M-Φ model as shown in Figure 11 is stipulated for evaluating seismic performance of follow steel bridge piers. The M-Φ model is decided based on the experimental results of bending roll pipes (Public Works Research Institute et al. 1997-1999). The point (Φ_a, M_a) of M-Φ model in Figure 11 corresponds to the point (δ_m , P_{max}) in Figure 6. The following procedure is an example how to set M-Φ model for follow steel bridge piers with circular sections.

1) A bilinear model as shown in Figure 12 is assumed as a stress-strain curve for setting the M-Φ model.
2) Allowable strain ε_a corresponding to the point (Φ_a, M_a) for steel piers with circular sections is obtained by using following equation.

$$\frac{\varepsilon_a}{\varepsilon_y} = 20 - 140R_t \tag{5}$$

where ε_y = yield strain of the steel used in the target steel pier.
Here, the above Eq. (5) can be applied if the following condition is satisfied.

$$0.03 \le R_t \le 0.08,\ \ 0.2 \le \overline{\lambda} \le 0.4,\ \ 0.0 \le N/N_y \le 0.2 \tag{6}$$

3) The points (Φ_{yc}, M_{yc}) and (Φ_{yt}, M_{yt}) are set when the strain in the center of plate thickness at the compression side or the tension side reaches the yield strain ε_y of steel for the first time respectively.
4) The point (Φ_a, M_a) is set when the strain in the center of plate thickness at the compression side reaches the allowable strain ε_a obtained from the Eq. (5) for the first time.

P_{max} was calculated by dividing M_a by the load height h and δ_a was calculated by utilizing the curvature distribution, ignoring shear deformation and geometric non-linearity effect.

Figure 13 show the comparison of experimental results of spiral steel pipes in this study ('●' in Figure 13) with the previous experimental results of bending roll pipes ('△' in Figure 13) and the analysis results by the previous seismic evaluation method. As shown in Figure 13, relatively good agreement between the experimental results of spiral steel pipes and analysis results by the previous seismic design method can be found. The relationship between the experimental results of spiral steel pipes and the analysis by the previous seismic evaluation method is basically similar to that between the previous experimental results of bending roll pipes and the analysis results. This fact indicates the possibility that the seismic performance of spiral steel pipes may be similar to that of bending roll pipes. In the future works, seismic performance of spiral steel pipes will be investigated in detail for developing seismic design method.

Conclusions

Cyclic loading experiments were conducted with spiral steel pipes as test specimens in order to grasp the seismic performance of spiral steel pipes. The results from experiments are concluded as follows.

・ The decrease in radius thickness ratio parameter leads to the increase in the maximum horizontal load and the horizontal displacement at the maximum horizontal load as well as bending roll pipes

・ Experimental results indicate a possibility that the seismic performance of spiral steel pipes may be similar to that of bending roll pipes and the previous seismic evaluation method for bending roll pipe piers may be applicable to spiral steel pipes

References

Kimura, Y., Ogawa, T. and Saeki, E. (2001). “The local buckling behavior of cold-formed circular tubes by different manufacturing process,” *Journal of Steel Construction Engineering,* Vol. 8, No. 29, 27-34 (in Japanese).

Japan Road Association (2002a). *Specifications for highway bridges, Part II: Steel bridges* (in Japanese).

Japan Road Association (2002b). *Specifications for highway bridges, Part V: Seismic Design* (in Japanese).

Public Works Research Institute of the Ministry of Construction and five other organizations (1997-1999). “Ultimate Limit State Design Method of Highway Bridges Piers under Seismic Loading”, *Cooperative Research Report* (in Japanese).

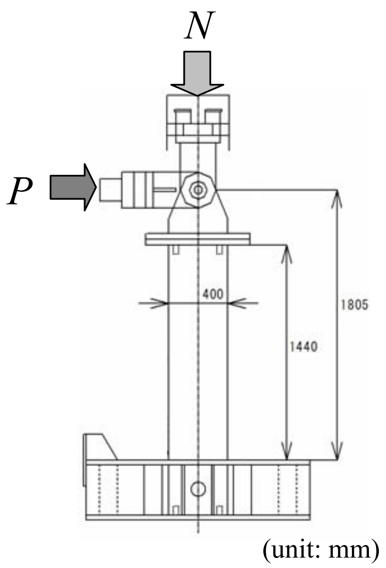

Figure 1 Test Specimen

Table 1 Parameters of Test Specimens

		A9-P	A7-P
Material (JIS)		SKK490	SKK490
Diameter (mm)		400	400
Thickness (mm)		9	7
Radius Thickness ratio		22.2	28.6
Area (cm^2)		111	86
Moment of inertia (cm^4)		21,138	16,691
The height of Loading point (mm)		1,805	1,805
Compressive Axial Force (kN)		522	408
Parameters calculated by nominal yield stress σ_{yN}	λ	0.33	0.32
	R_t	0.056	0.072
Parameters calculated by experimental yield stress σ_{yM}	σ_y (MPa)	470	409
	λ	0.40	0.37
	R_t	0.084	0.093

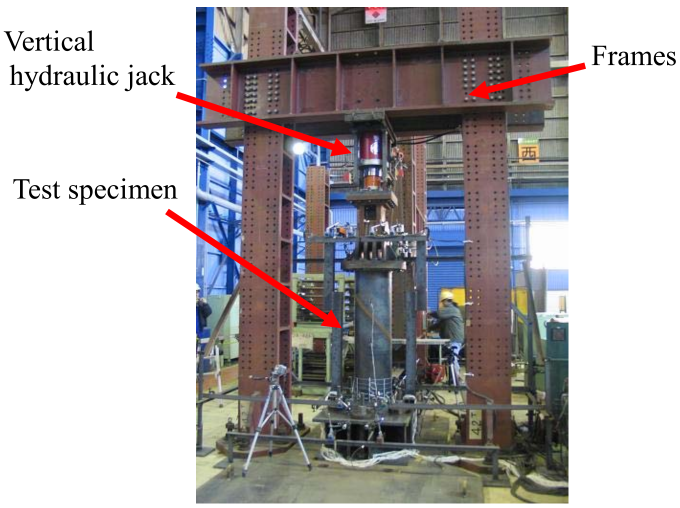

Figure 2 Test Setup

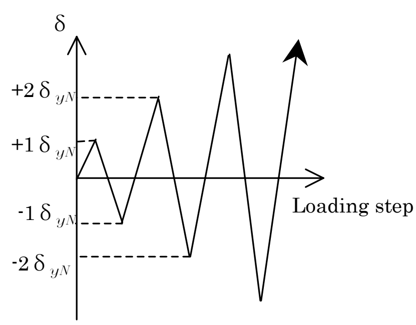

Figure 3 Cyclic Loading Pattern

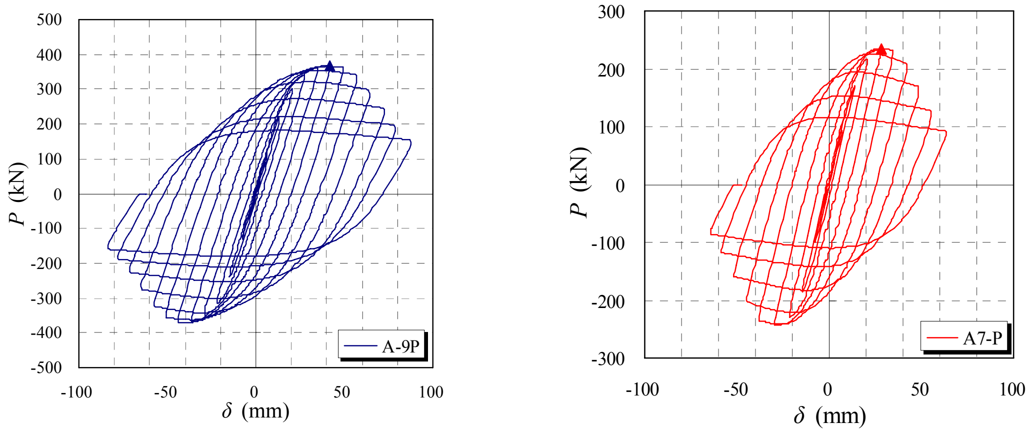

(A9-P) **(A7-P)**

Figure 4 *P-δ* Relationship

Table 2 Experimental Results

specimen	A9-P	A7-P
P_{yM} (kN)	248	165
P_{max} (kN)	369	235
P_{max}/P_{yM}	1.49	1.42
δ_{yM} (mm)	11.2	9.4
δ_{yEM} (mm)	14.7	12.2
δ_m (mm)	42.0	28.1
δ_m/δ_{yEM}	2.86	2.30

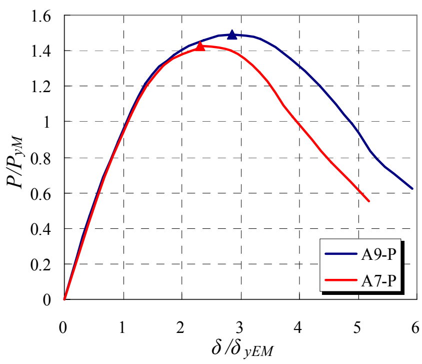

Figure 5 Envelop Curve

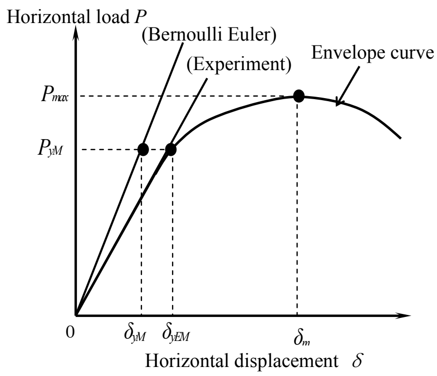

Figure 6 Definition of Symbols

Figure 7 Buckling Mode (A7-P)

Figure 8 Buckling Mode (A9-P)

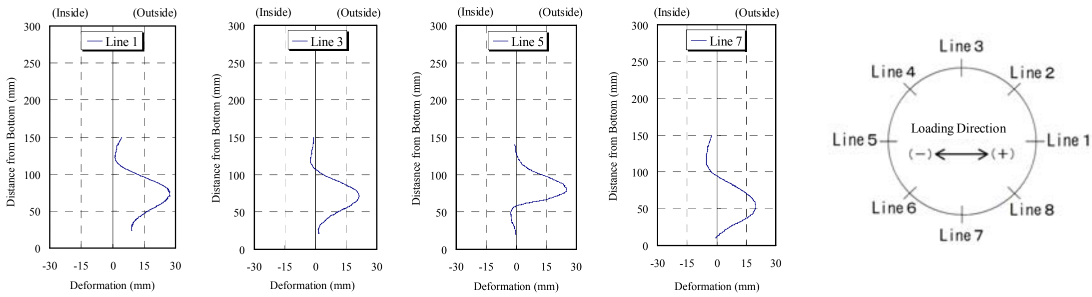

Figure 9 Distribution of Out-of-plane Deformation (A7-P)

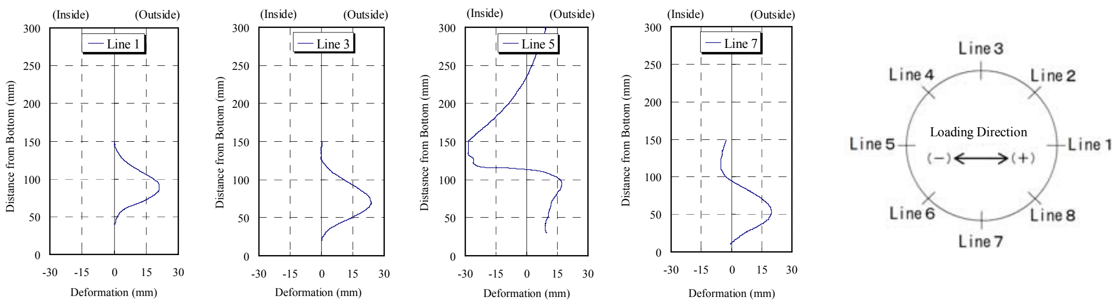

Figure 10 Distribution of Out-of-plane Deformation (A9-P)

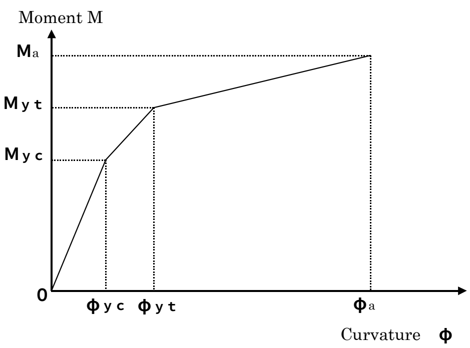

Figure 11 M-Φ Model

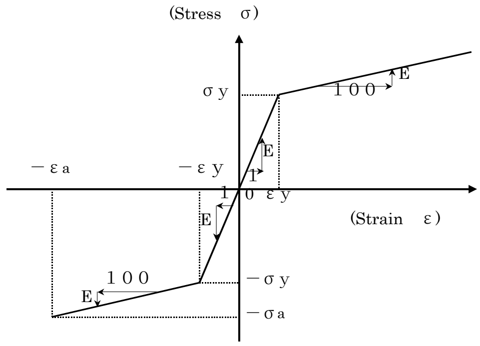

Figure 12 Stress-strain Relationship

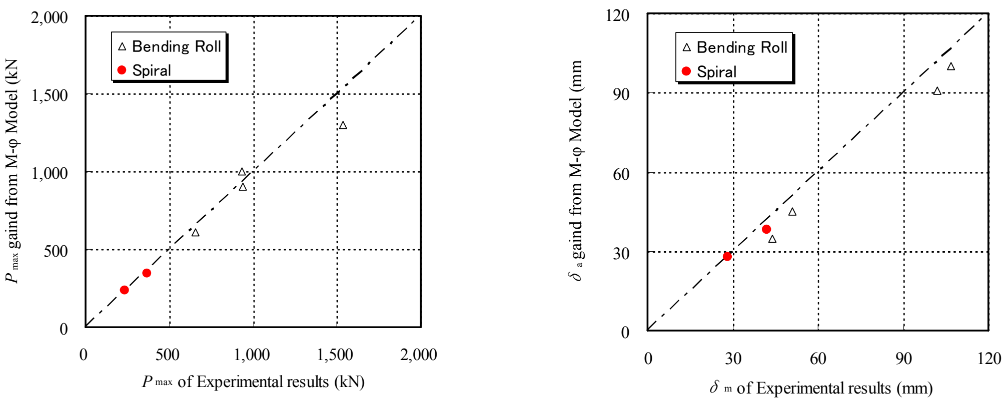

Figure 13 Comparison between Experimental Results and Analysis Results